

Molecular Aggregation of Annular Dinuclear Gold(I) Compounds Containing Bridging Diphosphine and Dithiolate Ligands

Shaw Shiah Tang,[†] Chen-Pin Chang,[†] Ivan J. B. Lin,^{*,†} Lin-Shu Liou,[‡] and Ju-Chun Wang^{*,‡}

Departments of Chemistry, Fu-Jen Catholic University, Hsinchuang, Taipei 242, Taiwan, ROC, and Soochow University, Taipei 111, Taiwan, ROC

Received June 18, 1996[⊗]

A series of annular dinuclear Au(I) complexes containing diphosphine ($R_2P(CH_2)_nPR_2$; $R = Me$, $n = 1$, dmpm; $R = Me$, $n = 2$, dmpe; $R = Ph$, $n = 1$, dppm; $R = Ph$, $n = 2$, dppe) and dithiolate ($dtc = S_2CNEt_2^-$, $i\text{-mnt} = S_2C_2(CN)_2^{2-}$) ligands were synthesized: $[Au_2(P\text{-}P)(S\text{-}S)]X$ ($S\text{-}S = dtc$: $P\text{-}P = dmpm$, $X = Cl$, **1**; $P\text{-}P = dppm$, $X = PF_6$, **2**; $P\text{-}P = dppe$, $X = PF_6$, **3**; $P\text{-}P = PPh_3$, $X = PF_6$, **4**) and $[Au_2(P\text{-}P)(S\text{-}S)]$ ($S\text{-}S = i\text{-mnt}$: $P\text{-}P = dmpm$, **5**; $P\text{-}P = dppm$, **6**; $P\text{-}P = dmpe$, **7**; $P\text{-}P = dppe$, **8**). Crystal structures of two complexes are reported. Pertinent crystallographic data: $[Au_2(dmpm)(i\text{-mnt})]$ (**5**), space group $Fdd2$, with $a = 19.574(3)$ Å, $b = 48.220(11)$ Å, and $c = 15.273(2)$ Å, $R = 0.0542$; $[Au_2(dppe)(i\text{-mnt})]$ (**8**), space group $P2_1/n$, with $a = 11.793(2)$ Å, $b = 19.607(2)$ Å, and $c = 15.349(2)$ Å, $R = 0.0448$. Each molecule has two gold atoms bridged by a dithiolate ligand on one side and a diphosphine ligand on the other side, thus forming an eight- or nine-membered ring digold complex. The tendency of the digold(I) compounds to aggregate through an intermolecular Au–Au interaction depends on the ligands. Among the structures determined, complex **5** forms a polymeric chain and compound **8** is monomeric. Molecular aggregation also occurs in solution. Concentration-dependent absorption spectra of Au–dte compounds suggest that an equilibrium between the monomer and dimer exists. Equilibrium constants corresponding to the intermolecular Au–Au interaction range from 38 to 137 M^{-1} with ΔH values of ~ 15 kcal/mol and ΔS values of ~ -35 to ~ -46 cal/(K mol). Concentration dependence of emission spectra of annular compounds in acetonitrile also supports association in solution. Emissions at ~ 400 – 440 nm assignable to spin-allowed metal-centered transitions from monomeric Au_2 at lower concentrations and dimeric Au_4 at higher concentrations are observed. Compounds **1**–**3** and **5**–**8** in the glass state having spin-forbidden dithiolate ligand to gold charge transfer (3LMCT) transitions give emission bands at ~ 550 nm. Compound **4** has a $S \rightarrow Au$ 3LMCT transition at 500 nm. ^{31}P variable-temperature NMR experiments were performed for **1**–**3**. The dynamic process is attributed to molecular aggregation through an intermolecular Au–Au interaction in solution. The activation energies are approximately 9 kcal/mol for **1** and **2**.

Introduction

One of the interesting properties of gold(I) complexes is a weak Au–Au interaction in the solid state.^{1,5–11} This weak interaction has an energy comparable to that of hydrogen bonds. The presence of such an interaction in gold(I) compounds has been attributed to the relativistic effect that results in the contraction of the 6s orbitals and the expansion of the 5d orbitals.² Many theoretical and experimental studies have been

carried out to investigate the Au–Au interaction.³ For example, calculations on $XAuPH_3$ suggested that the softness of the X ligand influences the Au–Au attraction.⁴ Experimentally, many gold(I) compounds with different ligands were prepared to probe this interaction. Among these gold(I) compounds, annular eight-membered digold(I) complexes are an ideal system for the study of intramolecular Au–Au interactions. Eight-membered digold(I) compounds, however, may or may not have intermolecular Au–Au interactions. For example, the complexes, $[Au(dithiolate)]_2^{n-}$ (dithiolate = $S_2CNR_2^-$,⁵ S_2COR^- ,⁶ $S_2P(OR)_2^-$,⁷ $S_2C_2(CN)_2^{2-}$,⁸ $R = \text{alkyl}$; $n = 0, 2$) are known to form a polymeric chain with both intra- and intermolecular Au–Au interactions. The complexes $[Au(diphosphine)]_2^{2+}$, with eight- to ten-membered dimetallacycle rings, however, have only intramolecular Au–Au interactions.⁹ The mixed-ligand compounds $[Au_2(\text{phosphine})_2(\text{thiolate})_2]$ promote intra- but not intermolecular Au–Au interactions with smaller rings.¹⁰ To our knowledge, only one example in which molecular association via Au–Au interactions occurs between eight-membered digold(I) compounds containing diphosphine has been reported.¹¹

[†] Fu-Jen Catholic University.

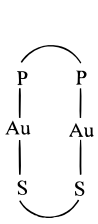

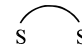
[‡] Soochow University.

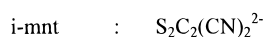
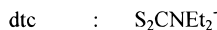
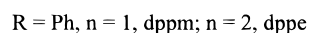
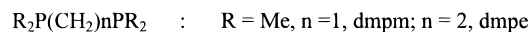
[⊗] Abstract published in *Advance ACS Abstracts*, April 1, 1997.

- (1) (a) Jiang, Y.; Alvarez, S.; Hoffmann, R. *Inorg. Chem.* **1985**, *24*, 749. (b) Vicente, J.; Chicote, M. T.; Llamas, I. S.; Jones, P. G.; Base, K. M.; Erdbrugger, C. F. *Organometallics* **1988**, *7*, 997. (c) Davila, R. M.; Elduquo, A.; Staples, R. J.; Harlass, M.; Fackler, J. P., Jr. *Inorg. Chim. Acta* **1994**, *217*, 45. (d) Bardaji, M.; Connelly, N. G.; Gimeno, M. C.; Jiménez, J.; Jones, P. G.; Laguna, A.; Laguna, M. *J. Chem. Soc., Dalton Trans.* **1994**, 1163.
- (2) (a) Pyykkö, P.; Desclaux, J. P. *Acc. Chem. Res.* **1979**, *12*, 276. (b) Pitzer, K. S. *Acc. Chem. Res.* **1979**, *12*, 271. (c) Pyykkö, P. *Chem. Rev.* **1988**, *88*, 563.
- (3) (a) Raptis, R. G.; Fackler, J. P., Jr.; Murray, H. H.; Porter, L. C. *Inorg. Chem.* **1989**, *28*, 4057. (b) King, C.; Wang, J. C.; Khan, Md. N. I.; Fackler, J. P., Jr. *Inorg. Chem.* **1989**, *28*, 2145. (c) Li, J.; Pyykkö, P. *Chem. Phys. Lett.* **1992**, *197*, 586. (d) Zhao, Y.; Pyykkö, P. *Angew. Chem., Int. Ed. Engl.* **1991**, *30*, 604.
- (4) Pyykkö, P.; Li, J.; Runeberg, N. *Chem. Phys. Lett.* **1994**, *218*, 133.
- (5) Heinrich, D. D.; Wang, J. C.; Fackler, J. P., Jr. *Acta Crystallogr.* **1990**, *C46*, 1447.
- (6) Weinstock, J.; Sutton, B. M.; Kuo, G. Y.; Walz, D. T.; Dimartino, M. J. *J. Med. Chem.* **1974**, *17*, 139.
- (7) Lawton, S. L.; Rohrbaugh, W. J.; Kokotailo, G. T. *Inorg. Chem.* **1972**, *11*, 2227.
- (8) Khan, Md. N. I.; Fackler, J. P., Jr.; King, C.; Wang, J. C.; Wang, S. *Inorg. Chem.* **1988**, *27*, 1672.

- (9) (a) Jaw, H. R. C.; Savas, M. M.; Rogers, R. O.; Mason, W. R. *Inorg. Chem.* **1989**, *28*, 1028. (b) Ludwig, W.; Meyer, W. *Helv. Chim. Acta.* **1982**, *65*, 934. (c) Kozelka, J.; Oswald, H. R.; Dübber, E. *Acta Crystallogr.* **1986**, *C42*, 1007. (d) Schmidbaur, H.; Wöhlleben, U. S.; Frank, A.; Hutter, G. *Chem. Ber.* **1977**, *110*, 2751.
- (10) (a) Davila, R. M.; Elduque, A.; Grant, T.; Staples, R. J.; Fackler, J. P., Jr. *Inorg. Chem.* **1993**, *32*, 1749. (b) Davila, R. M.; Staples, R. J.; Elduque, A.; Harlass, M.; Kyle, L.; Fackler, J. P., Jr. *Inorg. Chem.* **1994**, *33*, 5940. (c) Gimeno, M. C.; Jones, P. G.; Laguna, A.; Laguna, M.; Terroba, R. *Inorg. Chem.* **1994**, *33*, 3932.
- (11) Lin, I. J. B.; Lin, C. W.; Liu, L. K.; Wen, Y. S. *Organometallics* **1992**, *11*, 2227.

Chart 1

	compounds		
	1	dmpm	dtc
	2	dppm	dtc
	3	dppe	dtc
	4	(PPh ₃) ₂	dtc
	5	dmpm	i-mnt
	6	dppm	i-mnt
	7	dppe	i-mnt
	8	dmpe	i-mnt



Another interesting physical property exhibited by many gold(I) compounds is that they are usually luminous, especially when Au–Au interactions are present. Many papers illustrate the relationship between the emissive behavior and the Au–Au interaction.¹² Recently, Jones et al. reported that an Au–Au interaction is not a necessary condition for the luminescence of (phosphine)gold(I) thiolate compounds.¹³ Furthermore, the presence of Au–Au interactions does not significantly perturb the luminescence of these compounds. Another report by Forward et al., however, showed that the presence of Au–Au interactions affects the emission maximums of a series of monomeric gold(I) compounds containing phosphine and thiolate ligands.¹⁴

In this study of [Au₂(diphosphine)(dithiolate)] compounds (abbreviations and labelings are listed in Chart 1), the dithiolates were kept constant while the lengths of bridging carbon chains and substituents on phosphorus of the diphosphines were varied to assess the effect of different ligands on the degree of molecular association. Another goal in this study was to determine the influence of Au–Au interactions on the luminescent properties. Especially, we wanted to know whether molecular association can be observed in solution. The study of Au–Au interactions in solution provides insight into the nature of this weak interaction without the influence of crystal packing forces. The data may serve to aid in the design of Au(I) compounds for the treatment of arthritis and tumors.¹⁵

Experimental Section

Reagents. Hydrogen tetrachloroaurate trihydrate, bis(dimethylphosphino)methane, 1,2-bis(dimethylphosphino)ethane, bis(diphenylphosphino)methane, and 1,2-bis(diphenylphosphino)ethane were purchased from Aldrich, and, 2,2'-thiodiethanol was obtained from RDH. The compounds Au₂(dmpm)Cl₂ and Au₂(dmpe)Cl₂ were prepared by known methods.¹⁶

Apparatus. NMR data were obtained on a Bruker AC-F300 FT-NMR spectrometer operating at 300 MHz for ¹H and 121 MHz for

³¹P. For ¹H NMR spectra, SiMe₄ was used as the internal standard. The ³¹P{¹H} NMR spectra were referenced to external 85% H₃PO₄. Variable-temperature ³¹P{¹H} NMR data were obtained for 1–3 from +20 to –90 °C in CD₂Cl₂. Absorption and emission spectra were obtained by a Shimadzu UV-2101PC spectrophotometer and an Aminco-Bowman Series 2 fluorimeter, respectively. The lifetimes for the solution sample, in the nanosecond range, were measured by an Edinburgh FL900CD photon-counting system with a nitrogen lamp as the excitation source. The lifetimes for the glassy sample in the microsecond range were measured by the fluorimeter using the technique of pulse time delay.

Syntheses. (a) [Au₂(dmpm)(dtc)]Cl (1). To an acetone (60 mL) solution of Au₂(dmpm)Cl₂ (41 mg, 0.068 mmol) was added 17 mg of NaS₂CN(Et)₂ (0.102 mmol). After 16 h of stirring at room temperature, the acetone was evaporated under vacuum and the bright yellow solid that had formed was washed with water. Yellow crystalline samples were obtained by recrystallization from warm acetone. Yield: 63%. Mp: 153 °C. FAB/MS: 678.32 *m/z* (MW – Cl)⁺. Anal. Calcd for C₁₀H₂₄NP₂S₂ClAu₂: C, 16.80; H, 3.37; N, 2.00. Found: C, 16.10; H, 3.63; N, 2.08. ³¹P{¹H} NMR (dms_o-d₆): δ = 12.1 ppm. ¹H NMR (dms_o-d₆): δ = 3.87 ppm (q, 4H, ³J(HH) = 6.9 Hz, CH₂ of S₂CN(Et)₂); 2.97 ppm (t, 2H, ²J(HP) = 12.6 Hz, PCH₂); 1.83 ppm (t, 12H, ²J(HP) = 4.6 Hz, P(CH₃)₂); 1.23 ppm (t, 6H, ³J(HH) = 6.9 Hz, CH₃ of S₂CN(Et)₂).

(b) [Au₂(dppm)(dtc)]PF₆ (2). To an acetone (60 mL) solution of Au₂(dppm)Cl₂ (50 mg, 0.060 mmol) was added 15 mg of NaS₂CN(Et)₂ (0.090 mmol). After 16 h of stirring at room temperature, the acetone was evaporated under vacuum and the yellow solid that had formed was washed with water. The solid was then redissolved in CH₂Cl₂, followed by the addition of an ethanol solution of NH₄PF₆ to produce greenish yellow crystals. Yield: 81%. Mp: 180 °C dec. FAB/MS: 925.34 *m/z* (MW – PF₆)⁺. Anal. Calcd for C₃₀H₃₂NP₃S₂F₆Au₂: C, 36.44; H, 3.31; N, 1.39. Found: C, 36.93; H, 3.36; N, 1.30. ³¹P{¹H} NMR (CDCl₃): δ = 34.32 ppm. ¹H NMR (dms_o-d₆): δ = 7.83–7.4 ppm (m, 20H, PPh); 4.78 ppm (t, 2H, ²J(HP) = 13.8 Hz, PCH₂); 3.98 ppm (q, 4H, ³J(HH) = 6.7 Hz, CH₂ of S₂CN(Et)₂); 1.33 ppm (t, 6H, ³J(HH) = 6.8 Hz, CH₃ of S₂CN(Et)₂).

(c) [Au₂(dppe)(dtc)]PF₆ (3). This compound was prepared by the method described for compound 2. Pale green crystals were obtained. Yield: 62%. Mp: 215 °C dec. FAB/MS: 940.24 *m/z* (MW – PF₆)⁺. Anal. Calcd for C₃₁H₃₄NP₃S₂F₆Au₂: C, 34.30; H, 3.13; N, 1.30. Found: C, 33.60; H, 3.17; N, 1.40. ³¹P{¹H} NMR (CDCl₃): δ = 33.49 ppm. ¹H NMR (CDCl₃): δ = 7.83–7.50 ppm (m, 20H, PPh); 4.03 ppm (q, 4H, ³J(HH) = 7.1 Hz, CH₂ of S₂CN(Et)₂); 2.95 ppm (d, 4H, ²J(HP) = 12.3 Hz, P(CH₂)₂); 1.46 ppm (t, 6H, ³J(HH) = 7.1 Hz, CH₃ of S₂CN(Et)₂).

(d) [Au₂(PPh₃)₂(dtc)]PF₆ (4). This compound was prepared by the method described for compound 2. Pale green microcrystals were obtained. Yield: 40%. Mp: 189 °C dec. FAB/MS: 940.24 *m/z* (MW – PF₆)⁺. Anal. Calcd for C₄₁H₄₀NP₃S₂F₆Au₂: C, 40.63; H, 3.32; N, 1.16. Found: C, 39.53; H, 3.30; N, 1.20. ³¹P{¹H} NMR (CDCl₃): δ = 36.0 ppm. ¹H NMR (CDCl₃): δ = 7.53–7.26 ppm (m, 40H, PPh); 4.08 ppm (q, 4H, ³J(HH) = 7.1 Hz, CH₂ of S₂CN(Et)₂); 1.46 ppm (t, 6H, ³J(HH) = 7.1 Hz, CH₃ of S₂CN(Et)₂).

(e) [Au₂(dmpm)(i-mnt)] (5). To an acetone (50 mL) solution of Au₂(dmpm)Cl₂ (28 mg, 0.046 mmol) was added 10 mg of K₂(i-mnt) (0.046 mmol). After 24 h of stirring at room temperature, the acetone was removed by a vacuum evaporator. The yellow solid that had formed was washed with water thoroughly. Yellow crystalline samples were obtained by recrystallization from dimethyl sulfoxide. Yield: 62%. Mp: 231 °C dec. FAB/MS: 670.24 *m/z* (MW)⁺. Anal. Calcd for C₉H₁₄N₂P₂S₂Au₂: C, 16.09; H, 2.00; N, 4.10. Found: C, 16.39; H, 1.68; N, 3.95. ³¹P{¹H} NMR (dms_o-d₆): δ = 11.3 ppm. ¹H NMR (dms_o-d₆): δ = 3.08 ppm (t, 2H, ²J(HP) = 13.3 Hz, PCH₂), 1.82 ppm (d, 12H, ²J(HP) = 10.8 Hz, P(CH₃)₂).

(f) [Au₂(dppm)(i-mnt)] (6). To an acetone (50 mL) solution of Au₂(dppm)Cl₂ (75 mg, 0.093 mmol) was added 21 mg of K₂(i-mnt) (0.093 mmol). After 12 h of stirring at room temperature, the bright yellow resulting mixture was filtered and the pure, bright yellow solid obtained was washed with water. Yield: 73%. Mp: 246 °C dec. FAB/MS: 918.52 *m/z* (MW)⁺. Anal. Calcd for C₂₉H₂₂N₂P₂S₂Au₂·0.5(CH₃)₂CO: C, 38.66; H, 2.65; N, 2.96. Found: C, 38.68; H, 2.55; N, 2.99.

- (12) (a) Che, C. M.; Kwong, H. L.; Yam, V. W. W.; Cho, K. C. *J. Chem. Soc., Chem. Commun.* **1989**, 885. (b) Yam, V. W. W.; Lee, W. K. *J. Chem. Soc., Dalton Trans.* **1993**, 2097. (c) Che, C. M.; Kwong, H. L.; Yam, V. W. W.; Poon, C. K. *J. Chem. Soc., Dalton Trans.* **1990**, 3215. (d) Yam, V. W. W.; Lai, T. F.; Che, C. M. *J. Chem. Soc., Dalton Trans.* **1990**, 3747. (e) Assefa, Z.; McBurnett, B. G.; Staples, R. J.; Fackler, J. P., Jr.; Assmann, B.; Angermaier, K.; Schmidbauer H. *Inorg. Chem.* **1995**, *34*, 7518.
- (13) Jones, W. B.; Yuan, J.; Narayanaswamy, R.; Young, M. A.; Elder, R. C.; Bruce, A. E.; Bruce, M. R. *Inorg. Chem.* **1995**, *34*, 1996.
- (14) Forward, J. M.; Bohmann, D.; Fackler, J. P., Jr.; Staples, R. *Inorg. Chem.* **1995**, *34*, 6330.
- (15) Brown, D. H.; Smith, W. E. *Chem. Soc. Rev.* **1980**, *9*, 217.
- (16) Yam, V. W. W.; Choi, S. W. K. *J. Chem. Soc., Dalton Trans.* **1994**, 2057.

Table 1. Crystal Data for Compounds **5** and **8**

	5	8
formula	C ₉ H ₁₄ N ₂ P ₂ S ₂ Au ₂ · 0.5C ₂ H ₆ SO	C ₃₀ H ₂₄ N ₂ P ₂ S ₂ Au ₂ · CH ₂ Cl ₂
crystal size, mm ³	0.2 × 0.3 × 0.4	0.2 × 0.4 × 0.5
crystal system	orthorhombic	monoclinic
space group	<i>Fdd2</i>	<i>P2₁/n</i>
fw	1412.5	1015.4
<i>a</i> , Å	19.574(3)	11.793(2)
<i>b</i> , Å	48.220(11)	19.607(2)
<i>c</i> , Å	15.273(2)	15.349(2)
α, deg		
β, deg		112.13(1)
γ, deg		
<i>V</i> , Å ³	14416(4)	3287.9(6)
<i>Z</i>	32	4
<i>d</i> _{calc} , g/cm ³	2.603	2.051
μ, mm ⁻¹	16.722	9.325
no. of obsd reflns	1994	2989
criterion for observn	<i>F</i> > 4σ(<i>F</i>)	<i>F</i> > 4σ(<i>F</i>)
λ(radiation), ^a Å	0.710 73	0.710 73
<i>R</i> , ^b <i>R</i> _w ^c	0.0542; 0.0655	0.0448; 0.0519
<i>g</i>	0.002	0.001

^a Graphite-monochromated Mo Kα. ^b *R* = Σ(|*F*_o − |*F*_c||)/Σ(|*F*_o − |*F*_c||). ^c *R*_w = [Σw(|*F*_o − |*F*_c||)²]/Σw(|*F*_o − |*F*_c||)²]^{1/2}; *w* = [σ²(*F*_o) + *gF*_o²]⁻¹.

³¹P{¹H} NMR (dms-*d*₆): δ = 32.5 ppm. ¹H NMR (dms-*d*₆): δ = 7.74–7.35 ppm (m, 20H, PPh), 4.84 ppm (t, 2H, ²J(HP) = 13.3 Hz, PCH₂).

Compounds **7** and **8** were synthesized by procedures analogous to that described for compound **6**. Characterization data are given below.

(**g**) [Au₂(dmpe)(*i*-mnt)] (**7**). The pure greenish yellow solid was obtained by recrystallization from dimethyl sulfoxide. Yield: 69%. Mp: 201 °C dec. FAB/MS: 684.26 *m/z* (MW)⁺. Anal. Calcd for C₁₀H₁₆N₂P₂S₂Au₂: C, 17.50; H, 2.36; N, 4.09. Found: C, 17.85; H, 2.46; N, 3.94. ³¹P{¹H} NMR (dms-*d*₆): δ = 7.3 ppm. ¹H NMR (dms-*d*₆): δ = 2.28 ppm (d, 4H, ²J(HP) = 11.5 Hz, PCH₂), 1.66 ppm (d, 12H, ²J(HP) = 10.5 Hz, P(CH₃)₂).

(**h**) [Au₂(dppe)(*i*-mnt)] (**8**). Pale yellow crystals were obtained by recrystallization from CH₂Cl₂/hexane. Yield: 80%. Mp: 207 °C dec. FAB/MS: 932.54 *m/z* (MW)⁺. Anal. Calcd for C₃₀H₂₄N₂P₂S₂Au₂·0.5CH₂Cl₂: C, 37.57; H, 2.58; N, 2.87. Found: C, 39.11; H, 2.62; N, 2.74. ³¹P{¹H} NMR (dms-*d*₆): δ = 34.9 ppm. ¹H NMR (dms-*d*₆): δ = 7.83–7.57 ppm (m, 20H, PPh), 2.99 ppm (d, 4H, ²J(HP) = 13.2 Hz, P(CH₂)₂).

Crystal Structure Determinations: General Procedures. A crystal of ~0.4 mm dimensions was used for X-ray structural analysis. Cell constants were derived from least-squares refinement of 25 high-angle reflections (2θ up to 30°). Intensity data sets were collected using either the θ–2θ or ω scan mode on a Siemens P4 diffractometer equipped with graphite-monochromatized Mo Kα radiation (λ = 0.710 73 Å). Three standard reflections, were measured every 300 reflections, and only small (<5%) random variations were observed. An empirical absorption correction based on a series of Ψ scans was applied to the data. Lorentz and polarization corrections were also applied. The space groups were unambiguously revealed from systematic absences. The structures were solved by the heavy-atom method using the SHELXTL-PLUS software package.¹⁷

Gold atom positions were revealed on a Patterson map. All other non-hydrogen atoms were located from subsequent Fourier difference syntheses. H atom positions were placed in calculated positions (C–H = 0.960 Å) with fixed displacement parameters (*U* = 0.08 Å²) but were not included in least-squares refinements. The structures were refined by the full-matrix least-squares method. Σw(|*F*_o − |*F*_c||)² was minimized, where *w* = 1/[σ²(*F*_o) + *gF*_o²]. The crystal data for these two compounds are listed in Table 1.

Results and Discussion

Syntheses. Au(I) compounds with various combinations of diphosphines (dmpm, dmpe, dppm, and dppe) and dithiolates (*i*-mnt and dtc) were prepared by the reaction of Au₂(diphosphine)Cl₂ with dithiolates. The only missing compound,

Table 2. Selected Bond Lengths (Å) and Angles (deg) of [Au₂(dmpm)(*i*-mnt)], **5**

Au(1)–Au(2)	2.925(3)	Au(1)–Au(3)	3.095(3)
Au(2)–Au(4A)	3.171(3)	Au(3)–Au(4)	2.893(3)
Au(1)–S(1)	2.320(12)	Au(1)–P(1)	2.268(13)
Au(2)–S(2)	2.307(14)	Au(2)–P(2)	2.253(13)
Au(2)–Au(1)–Au(3)	173.5(1)	Au(1)–Au(3)–Au(4)	103.3(1)
Au(1)–Au(2)–Au(4A)	119.5(1)	Au(3)–Au(4)–Au(2A)	167.9(1)
S(1)–Au(1)–P(1)	176.3(5)	S(2)–Au(2)–P(2)	174.7(5)

Table 3. Selected Bond Lengths (Å) and Angles (deg) of [Au₂(dppe)(*i*-mnt)], **8**

Au(1)–Au(2)	2.850(1)	Au(1)–P(1)	2.258(4)
Au(1)–S(1)	2.312(4)	Au(2)–P(2)	2.276(4)
Au(2)–S(2)	2.324(4)		
P(1)–Au(1)–S(1)	175.6(2)	P(2)–Au(2)–S(2)	175.5(2)

[Au₂(dmpe)(dtc)]Cl, is unstable. Although the FAB/MS spectrum suggests the formation of this compound, attempts of purification in solution produce [Au₂(dtc)₂], which was identified by X-ray diffraction techniques. Recently, the similar compounds [Au₂(dppm)(S₂COR)]ClO₄ (R = Me, Et), which were prepared by the reaction of [Au₂(dppm)₂](ClO₄)₂ with [Au₂(S₂COR)₂], were reported.¹⁸ We examined a mixture of [Au₂(dppm)₂]Cl₂ and [Au₂(dtc)₂] in CDCl₃ by ³¹P NMR spectroscopy; the only species observed was [Au₂(dppm)(dtc)]Cl.

Crystal Structures. Selected bond lengths and angles of Au–*i*-mnt compounds **5** and **8** are given in Tables 2 and 3, respectively. Coordination geometries around each gold atom in the two compounds are identical. All of the P–Au–S angles are close to linear, and the Au–P and Au–S bonds are comparable to reported values.¹⁰ Both molecules have short intramolecular Au–Au interactions irrespective of whether they are eight- or nine-membered dimetallacycles. These two compounds differ in their degree of molecular aggregation, which depends on the substituents and the bridging carbon chain length of the diphosphine ligands. Compound **5**, which has a dmpm ligand, forms a one-dimensional polymer in the solid state (Figure 1a). The molecular structure of one of the unique units of **5** is shown in Figure 1b. Viewed along the crystallographic *c* axis, compound **5** shows a novel helical configuration (Figure 2). The nine-membered-ring compound **8** having a dppe ligand is monomeric and has no short-range intermolecular Au–Au contact (Figure 3). **1** has a polymeric crystal structure, **2** a tetrameric, and **3** a monomeric. This result was published elsewhere.¹⁹

Electronic Absorption. The absorption spectra of **1–4** in acetonitrile have a common band around 270 nm, with an extinction coefficient (ε) on the order of ~10⁴ M⁻¹ cm⁻¹, mainly a dtc ligand involved transition. Compounds **2–4** show an additional shoulder at 310 nm (ε ~ 10³ M⁻¹ cm⁻¹) due to the presence of phenyl groups. Careful examination of the spectra of **1–3** shows another low-energy (LE) shoulder at 355, 365, and 367 nm, respectively. These bands are concentration dependent. The spectrum of **2** showing the nonlinear growth of the LE bands is given in Figure 4. The other two spectra are given in the Supporting Information. If we assume that a monomer is in equilibrium with its corresponding dimer which gives rise to the LE band, eq 1 can be derived, where [M]₀ is

$$\frac{[M]_0}{A_2^{1/2}} = \frac{1}{(\epsilon_2 K b)^{1/2}} + \frac{2A_2^{1/2}}{\epsilon_2 b} \quad (1)$$

the initial concentration of the monomer, *b* is the cell path length,

(18) Bardaji, M.; Jones, P. G.; Laguna, A.; Laguna, M. *Organometallics* **1995**, *14*, 1310.

(19) Tang, S. S.; Lin, I. J. B.; Liou, L. S.; Wang, J. C. *J. Chin. Chem. Soc.* **1996**, *43*, 327.

(17) SHELXTL-Plus, Release 4.2; Siemens Analytical X-ray Instruments Inc: Karlsruhe, Germany, 1991.

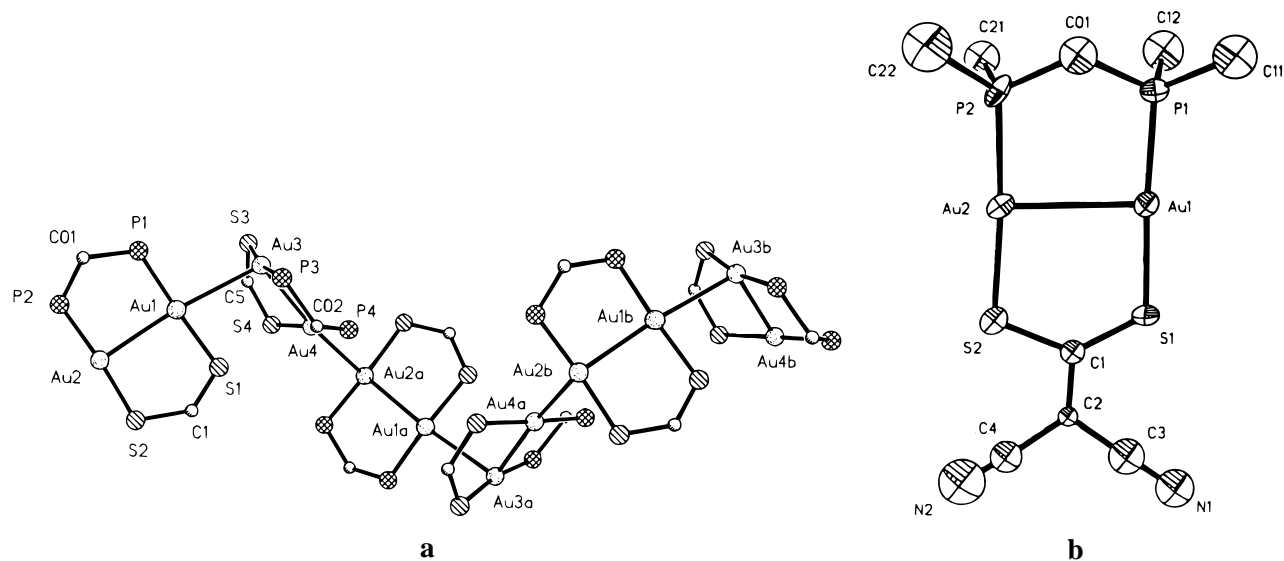


Figure 1. (a) Perspective view of $[\text{Au}_2(\text{dmpm})(i\text{-mnt})]$ (**5**) showing the $\text{Au}_2(\text{PCP})(\text{SCS})$ rings and the Au–Au chains. Six molecules are shown to illustrate the progression of association. The methyl groups of the dmpm ligand and $\text{C}(\text{CN})_2$ group of the *i*-mnt ligand are omitted for clarity. (b) Perspective view of the molecular structure and labeling scheme for $[\text{Au}_2(\text{dmpm})(i\text{-mnt})]$ (**5**). Only one of the unique molecules is shown.

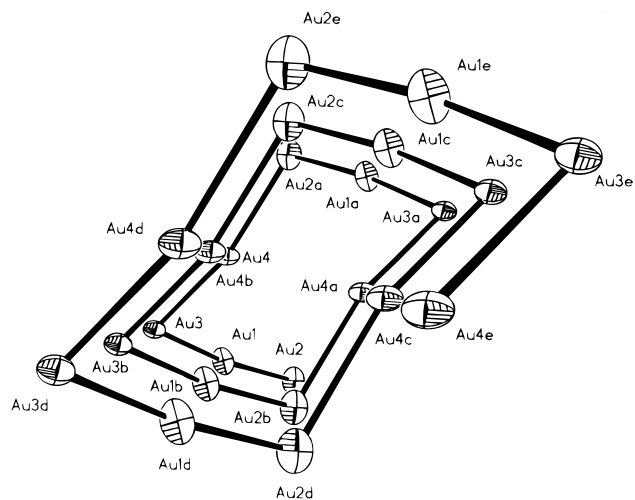


Figure 2. Perspective view of $[\text{Au}_2(\text{dmpm})(i\text{-mnt})]$ (**5**), viewed along the *c* axis. Only gold atoms are shown.

A_2 is the absorbance of the dimer, and ϵ_2 is the extinction coefficient of the dimer. A plot of $[\text{M}]_0/A_2^{1/2}$ vs $A_2^{1/2}$ gives a straight line for compounds **1–3** (Figure 5), suggesting that the above assumption is correct. Since up to the concentration of 10^{-2} M (the limiting solubility in this system) these plots are linear and no additional bands beyond 370 nm were observed, we believe the concentration of trimer is negligible. This result may be understood by repulsions arising from the flexible rings in the compounds. From the slope of these plots, the respective extinction coefficients of 8592 ± 1156 , 16103 ± 1885 , and $6265 \pm 973 \text{ M}^{-1} \text{ cm}^{-1}$ for dimers **1–3** were obtained. From the intercepts of these plots, equilibrium constants of 137 ± 40 (for **1**), 38 ± 4 (for **2**), and 61 ± 10 (for **3**) M^{-1} at room temperature were obtained. The most likely origin of these LE bands is a metal-centered (MC) transition involving the Au_4 unit of the dimer. The ~ 360 nm absorptions originating from the Au_4 MC transition are compared to the 315 nm absorption band originating from the Au_3 MC transition in $[\text{Au}_3(\text{PMe}_2\text{CH}_2\text{PMeCH}_2\text{PMe}_2)_2]^{3+}$ and $\sim 269\text{--}293$ nm absorption maximums originating from the Au_2 MC transition in $[\text{Au}_2(\text{dmpm})_2]^{2+}$ and $[\text{Au}_2(\text{dpmm})_2]^{2+}$.^{12a,d} The red shift from a Au_2 unit to Au_3 and then to a Au_4 unit is consistent with the correlation between the nuclearity number and the metal-centered transition energy.^{12d} From the equilibrium constants at different temperatures, ΔH values of

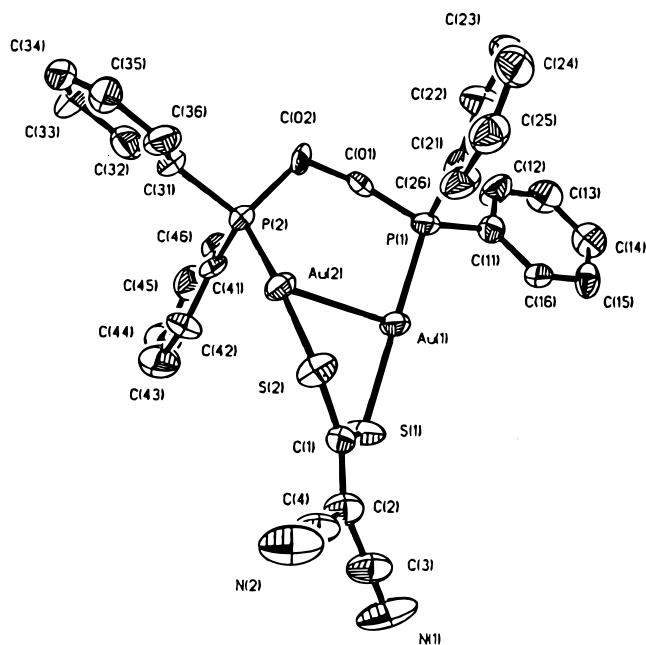


Figure 3. Perspective view of the molecular structure and labeling scheme for $[\text{Au}_2(\text{dppe})(i\text{-mnt})]$ (**8**).

14 ± 3 and 15 ± 10 kcal/mol and ΔS values of -35 ± 3 and -46 ± 35 cal/(K mol) corresponding to the intermolecular Au–Au bond formation are obtained for compounds **2** and **3**, respectively. Although aggregation of gold(I) compounds in the solid state is well-known, aggregation in solution is very rare²⁰ and no thermodynamic data have been reported. This is the first example showing that “auriophilicity” also operates between annular digold compounds in solution. The strengths of this intermolecular Au–Au interaction are in the upper value range, as estimated by Schmidbaur^{21a} and Hawthorne.^{21b} The negative ΔS values are consistent with an association process and are comparable to those reported for the association of Ni(β -diketonates)₂ in solution.²² It is important to note that although **3** does not aggregate in the solid state, it does so in solution. For compound **4**, up to the concentration of 1.0×10^{-2} M, no apparent peak at the LE end is observed, suggesting

(20) (a) Toronto, D. V.; Weissbart, B.; Tinti, D. S.; Balch, A. L. *Inorg. Chem.* **1996**, *35*, 2484. (b) Balch, A. L.; Fung, E. Y.; Olmstead, M. M. *J. Am. Chem. Soc.* **1990**, *112*, 5181.

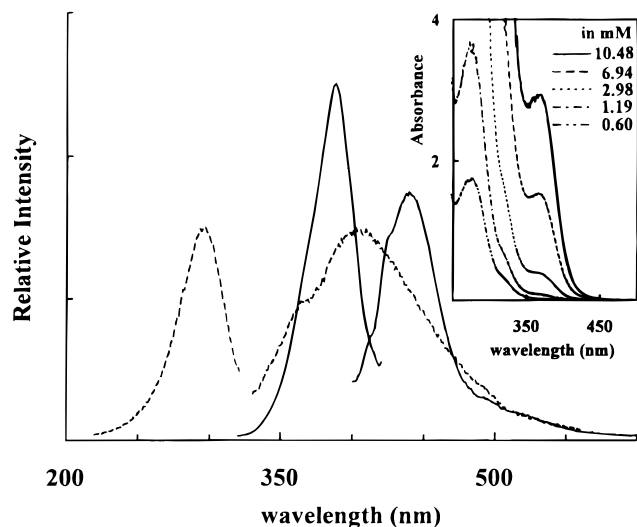


Figure 4. Concentration-dependent excitation and emission spectra of $[\text{Au}_2(\text{dppm})(\text{dtc})]\text{PF}_6$ (**2**) in acetonitrile: (a) 1.4×10^{-3} (—) and (b) 1.1×10^{-5} (---) M. Inset: Concentration-dependent absorption spectra of $[\text{Au}_2(\text{dppm})(\text{dtc})]\text{PF}_6$ (**2**) in acetonitrile.

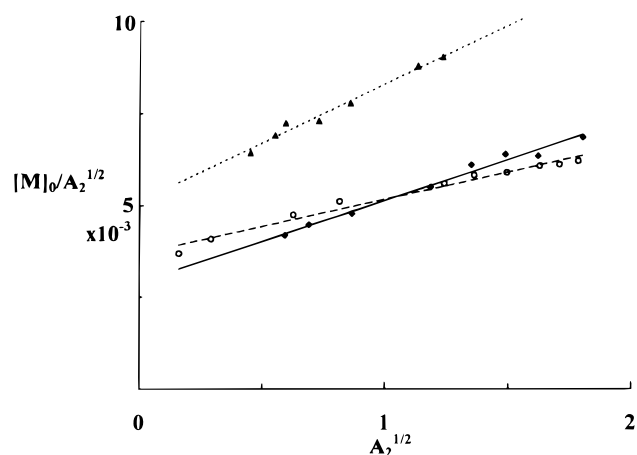


Figure 5. Plots of $[\text{M}]_0/\text{A}_2^{1/2}$ vs $\text{A}_2^{1/2}$ for (a) $[\text{Au}_2(\text{dmpm})(\text{dtc})]\text{Cl}$ (**1**) (—) over the range $1.2 \times 10^{-2} \text{ M} > [\text{M}]_0 > 2.5 \times 10^{-3} \text{ M}$ in acetonitrile (b) $[\text{Au}_2(\text{dppm})(\text{dtc})]\text{PF}_6$ (**2**) (---) over the range $1.1 \times 10^{-2} \text{ M} > [\text{M}]_0 > 5.9 \times 10^{-4} \text{ M}$ in acetonitrile, and (c) $[\text{Au}_2(\text{dppe})(\text{dtc})]\text{PF}_6$ (**3**) (···) over the range $1.1 \times 10^{-2} \text{ M} > [\text{M}]_0 > 2.9 \times 10^{-3} \text{ M}$ in acetonitrile.

that **4** remains as a monomer in solution. For compounds **5–8**, the MC transitions are interfered with by a strong intraligand transition, which happens to be in the range 250–400 nm. Therefore no obvious concentration dependent behavior was observed.

Emission. Compounds **1–3** and **5–8** luminesce at room temperature in acetonitrile solution. Compounds **1–8** are also luminous at 77 K in the glass state. Luminescent data for these gold(I) phosphine thiolate compounds are summarized in Table 4. To understand the nature of the emission behavior, we will discuss the emission spectra under three categories. In the first category, the emission maximums appear in the vicinity of 400–440 nm and are concentration dependent. The second category has emission maximums at ~ 500 nm and has simple excitation spectra at ~ 395 nm. The third one has emission maximums in the ~ 520 – 576 nm region and has complicated excitation profiles ranging from 300 to 480 nm.

The spectra that belong to the first category are those of annular digold compounds **1–3** and **5–8** in acetonitrile at 298

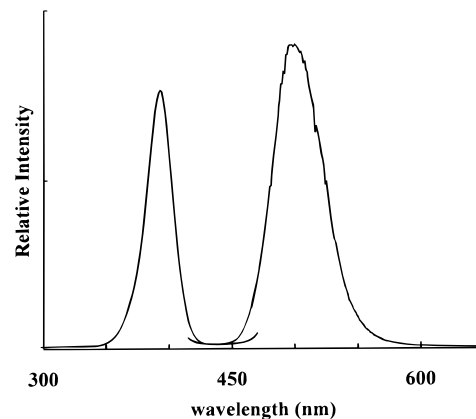


Figure 6. Excitation and emission spectra of $[\text{Au}_2(\text{PPh}_3)_2(\text{dtc})]\text{PF}_6$ (**4**) in acetonitrile at 77 K.

Table 4. Emission Data for Compounds **1–8** in Acetonitrile at 77 K

compd	no.	λ_{em} , nm	compd	no.	λ_{em} , nm
$[\text{Au}_2(\text{dmpm})(\text{dtc})]\text{Cl}$	1	564 ^a	$\text{Au}_2(\text{dmpm})(i\text{-mnt})$	5	558 ^a
$[\text{Au}_2(\text{dppm})(\text{dtc})]\text{PF}_6$	2	540 ^a	$\text{Au}_2(\text{dppm})(i\text{-mnt})$	6	558 ^a
$[\text{Au}_2(\text{dppe})(\text{dtc})]\text{PF}_6$	3	520 ^a	$\text{Au}_2(\text{dmpe})(i\text{-mnt})$	7	540 ^a
$[\text{Au}_2(\text{PPh}_3)_2(\text{dtc})]\text{PF}_6$	4	500 ^b	$\text{Au}_2(\text{dppe})(i\text{-mnt})$	8	576 ^a

^a Excitation at 300–480 nm. ^b Excitation at 395 nm.

K. The open-ring compound **4** does not luminesce in acetonitrile at 298 K. In this category, usually two sets of concentration-dependent excitation and emission maximums can be located. Although some of the spectra are interfered with by Raman scattered light, compounds **2**, **3**, and **8** show the most easily recognizable excitation and emission sets at different concentrations and will be illustrated first. The emission and excitation spectra of compound **2** in acetonitrile at 298 K at a concentrations of 1.4×10^{-3} and 1.1×10^{-5} M are shown in Figure 4. The set that appears at a higher concentration has an emission at 440 nm with an excitation at ~ 370 nm, and the set that appears at a lower concentration has an emission at 400 nm and an excitation at 295 nm. Correspondingly, compound **3** has an emission at 430 nm (excitation maximum at ~ 370 nm at 2.0×10^{-3} M) and another emission at 405 nm (excitation maximum at 300 nm at 1.3×10^{-4} M) (see supplementary material). Compound **1** at higher concentration (4.8×10^{-4} M) has emission and excitation maximums at ~ 410 and ~ 350 nm, respectively. At lower concentration (1.0×10^{-6} M), the emission maximums depend on the excitation wavelength. With excitation at ~ 350 nm, an emission maximum at ~ 410 nm is observed, while excitation at ~ 295 nm gives an emission at ~ 360 nm with long tailing (see supplementary material). Similarly, compound **8** has two emission bands at ~ 420 nm (excitation maximum at 350 nm at 7.0×10^{-5} M) and at 410 nm (excitation maximum at 290 nm at 1.0×10^{-5} M) (see supplementary material). The shift of the emission is less sensitive than that of the Au–dtc compounds. For other Au–*i*-mnt compounds, sets of emission and excitation bands are less well resolved. Nevertheless concentration- and excitation-wavelength-dependent emission spectra can be observed.

The second category includes the spectrum of compound **4** in acetonitrile glass at 77 K: an emission at 500 nm with a simple excitation at 395 nm (Figure 6). The emission and excitation spectra in this category resemble those of dinuclear gold(I) phosphine thiolate compounds reported by Bruce.¹³

In the third category are the spectra of annular digold compounds **1–3** and **5–8** in glass at 77 K. The emission and excitation spectra of **1** in acetonitrile glass at 77 K are shown in Figure 7. The emission spectrum having a maximum at 564 nm (glass at 77 K, lifetime $> 30 \mu\text{s}$) is insensitive to the change

(21) (a) Schmidbaur, H.; Graf, W.; Müller, G. *Angew. Chem., Int. Ed. Engl.* **1988**, *27*, 417. (b) Harwell, D. E.; Mortimer, M. D.; Knobler, C. B.; Anet, F. A. L.; Hawthorne, M. F. *J. Am. Chem. Soc.* **1996**, *118*, 2679.
(22) (a) Fackler, J. P., Jr.; Cotton, F. A. *J. Am. Chem. Soc.* **1961**, *83*, 3775. (b) Cotton, F. A.; Fackler, J. P., Jr. *J. Am. Chem. Soc.* **1961**, *83*, 2818.

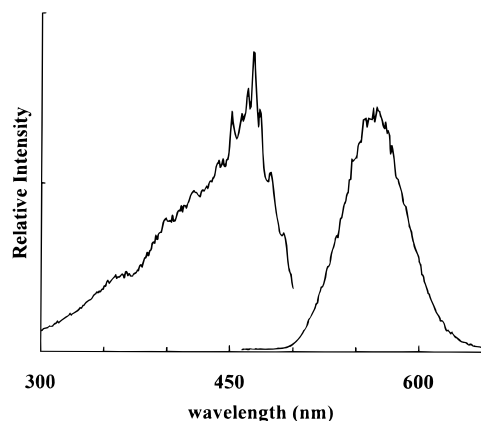


Figure 7. Excitation and emission spectra of $[\text{Au}_2(\text{dmpm})(\text{dtc})]\text{Cl}$ (**1**) in acetonitrile at 77 K.

of excitation wavelength from 300 to 480 nm. The excitation profile has a small maximum at the high-energy end (350 nm) and has structured bands at the LE end (~ 465 nm). Emission and excitation spectra of Au-dtc compounds **2** and **3** are similar to those of **1** in glass, and the data are listed in Table 4. For the Au-*i*-mnt compounds **5–8**, the samples in acetonitrile glass at 77 K have emission properties similar to those of Au-dtc compounds, and the data are listed in Table 4.

Possible sources of emissions observed in this work are (1) intraligand (IL) $\pi-\pi^*$ transitions involving phenyl ring or dithiolate ligands, (2) a metal-centered (MC) transition, and (3) a charge transfer (CT) transition involving either a metal to ligand (ML) or a ligand to metal (LM) transfer. Among these, an IL transition is the least likely to be responsible for the observed emission for the following reasons: (1) compounds **1**, **5**, and **7** do not have phenyl rings on the phosphine ligands, yet they luminesce, (2) Na(dtc) is not luminescent in the visible range, and (3) $\text{K}_2(i\text{-mnt})$ only luminesces at 77 K with a maximum at 640 nm. The above reasoning leaves the MC and CT transitions as the two most likely assignments. From the later arguments, it will be clear that both of these two transitions are present in our system. Among the two possible CT transitions, only LMCT will be considered, by following the arguments given in reports on other gold(I) phosphine thiolate compounds.

Since the excitation profiles of the first category are dramatically different from the ones in the third category, the natures of these emissions should be different. Comparing the concentration dependence of the emission and absorption spectra for compounds **1–3**, we note that the excitation maximums (~ 370 nm) responsible for the emission (λ_{max} at $\sim 430\text{--}440$ nm) at higher concentration are at about the same locations and are assignable to Au_4 MC transitions arising from the dimer in the absorption spectra. We therefore suggest that the emissions at higher concentration at $\sim 430\text{--}440$ nm originate from Au_4 MC transitions of the dimers. The relatively simple excitation profile for **2** or **3** is consistent with a MC transition. The excitation maximums (at ~ 290 nm) responsible for the emission (λ_{max} at ~ 400 nm) at lower concentration are comparable to those reported for Au_2 MC transitions in $[\text{Au}_2(\text{diphosphine})_2]^{2+}$ compounds.^{3b,9a,12a} Therefore, the emissions at lower concentration at ~ 400 nm are likely to originate from Au_2 MC transitions of the monomers. Both absorption and emission spectral studies suggest the existence of an equilibrium between the monomer and the dimer. Higher concentration favors the dimer, and lower concentration favors the monomer. Concentration-dependent emission behaviors of compounds **1** and **8** are similar to those of **2** and **3**, as are the natures of the emissions. The Au_2 and Au_4 MC transitions observed in this category are believed to

be spin-allowed transitions from singlet excited states for the following reasons: (1) The Stokes shift from excitation maximums are not large ($10^2\text{--}10^3$ cm^{-1}). (2) The luminescence lifetimes are in the nanosecond range. (3) Other reported spin-forbidden Au_2 and Au_3 MC transitions are at much lower energies (with maximums at $\sim 500\text{--}580$ nm) and have lifetimes in the microsecond range.^{12a,d} To the best of our knowledge, this is the first time that ^1MC transitions have been observed. This is also the first time that two ^1MC transitions (with Au_2 and Au_4 units) have been observed. The red shift of emission and excitation maximums from Au_2 to Au_4 is parallel to the behavior of the absorption spectra observed in this work and that of others.^{12d} Although other Au-*i*-mnt compounds are also concentration dependent, the excitation and emission spectra are less well resolved. One possibility is that the shift of emission for Au-*i*-mnt compounds is not sensitive to dimerization. Rather unexpectedly, although compounds **3** and **8** with dppe ligands are monomeric in the solid state, dimeric species can be identified in solution. Possibly, the crystal packing forces disfavor the dimerization of the more flexible nine-membered-ring compounds (**3** and **8**). In solution, this factor is not involved; hence, dimerization is possible.

The second category are the simplest excitation and emission spectra discussed in this work. The emission at ~ 500 nm is a spin-forbidden transition because (1) the luminescence lifetimes are relatively long (>20 μs) and (2) up to the concentration of 10^{-2} M, the corresponding excitation band at ~ 395 nm cannot be observed in the absorption spectrum, suggesting that the excitation is a spin-forbidden transition. The emissions are therefore spin-forbidden transitions from triplet to singlet states. The origin of emissions in this category is not a MC transition because the excitation maximum at ~ 395 nm is not in the vicinity of absorption arising from a MC transition. The origin of emissions is also not a dithiolate ligand to metal LMCT transition because the excitation profiles do not show fine structures arising from dithiolate ligands. We believe that the nature of emissions in this category is that of a $S \rightarrow \text{Au } ^3\text{LMCT}$ excited state, as was suggested for a series of dinuclear gold(I) phosphine thiolate compounds by Bruce.¹³ The difference in emission behavior between compound **4** and compounds in the third category is likely due to the open ring structure adopted by **4**. The two bulky PPh_3 ligands probably distort the compound, rendering the charge transfer from the whole ligand unfavorable.

In the third category, the contrast between complicated excitation profiles and simple emission bands suggests that the former contain several excited states. At the LE end, fine structures with spacings of ~ 1410 and ~ 460 cm^{-1} for some Au-*i*-mnt compounds and ~ 1460 and ~ 470 cm^{-1} for some Au-dtc compounds can be found. According to the analysis of emission and absorption spectra of $\text{Au}_2(\text{PPh}_3)_2(i\text{-mnt})$ (**9**) reported recently, resolved vibronic structure with a progression of 1410 cm^{-1} is attributed to a C=C bond vibration and a progression of 480 cm^{-1} is due to a Au-S vibration.²³ The fine structures observed in this category therefore involve gold-dithiolate stretching. The absorption spectra of **1–8** do not have a band at ~ 450 nm. The structured band observed at ~ 450 nm in the excitation spectra is likely due to a spin-forbidden transition.

The insensitivity of emission spectra to excitation wavelengths from ~ 300 to 480 nm is similar to that of **9**. Therefore, emissions of our annular digold compounds are likely to arise from a $^3\text{LMCT}$ excited state, primarily a dithiolate to gold transition, similar to the assignment given for **9**. Emissions of two related dinuclear¹³ and mononuclear¹⁴ gold compounds

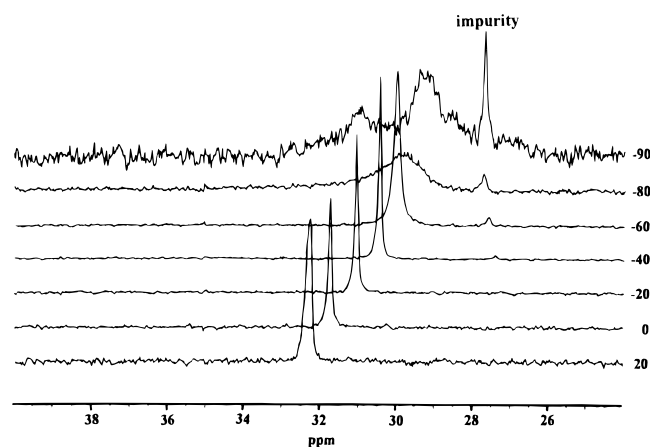


Figure 8. Variable-temperature ^{31}P NMR spectra of $[\text{Au}_2(\text{dppm})(\text{dtc})]\text{PF}_6$ (**2**) in CD_2Cl_2 from -90 to $+20$ $^\circ\text{C}$.

having both phosphine and thiolate ligands were also assigned as a $^3\text{LMCT}$, but primarily from the sulfur orbital and not from a π orbital associated with the phenyl group on the thiolates. The reported dinuclear gold compounds having relatively sharp excitation spectra at ~ 385 nm are different from the ones reported in this work (except for that of **4**).¹³ The related mononuclear gold compounds, especially those with the 1,3,5-triaza-7-phosphaadamantanetriylphosphine (TPA) ligand, showed no π involvement profiles from 250 to 400 nm.¹⁴ Apparently, the nature of the emission of annular dinuclear gold compounds with *i*-mnt and dtc ligands differs from that of simple thiolates such as alkanethiolates or benzenethiolates.

Variable-Temperature ^{31}P NMR Studies. The ^{31}P NMR spectra for compounds **1–8** reveal only one peak at room temperature, consistent with the equivalency of phosphorus atoms in each binuclear compound in solution. In order to see whether molecular association also occurs in solution, the ^{31}P variable-temperature NMR (VT-NMR) spectra in CD_2Cl_2 were recorded for compounds **1–3**, which are reasonably soluble in dichloromethane. The ^{31}P VT-NMR spectra of compound **2** from $+20$ to -90 $^\circ\text{C}$ are shown in Figure 8. At -90 $^\circ\text{C}$, two major broad signals of unequal intensity at 29.3 and 31.0 ppm were observed. At -80 $^\circ\text{C}$, the two broad peaks coalesced to one broad band at 29.8 ppm. When the temperature was raised to -40 $^\circ\text{C}$, the peak at 29.8 ppm sharpened. The ^{31}P NMR spectra of compound **1** are also temperature dependent. At -60 $^\circ\text{C}$, two broad signals at 10.6 and 15.5 ppm with unequal intensities were observed. The coalescence temperature was observed at -40 $^\circ\text{C}$. For compound **3**, we were unable to observe the splitting of the single peak; the peak however became very broad at -90 $^\circ\text{C}$. Using a coalescence temperature of -40 $^\circ\text{C}$ and a peak separation of 588 Hz at the low temperature,²⁴ we were able to calculate the activation energy of the dynamic process responsible for VT-NMR spectra of **1** as ~ 10 kcal/mol.²⁵ The activation energy for the same dynamic process of compound **2** is ~ 9 kcal/mol²⁵ (coalescence temperature of -80 $^\circ\text{C}$, peak separation of 204 Hz²⁴).

It is likely that the NMR temperature dependence of compounds **1** and **2** also arises from molecular association in solution. The line shape changes of ^{31}P VT-NMR for compounds **1** and **2** are similar to those reported by Narayanaswamy et al, in which interconversion between Au–Au-bonded and nonbonded isomers was proposed for the acyclic compound $[\text{Au}_2(\text{dppm})(\text{SC}_6\text{H}_4\text{CH}_3)_2]$ and ring inversion was proposed for the 11- and 13-membered-ring compounds $[\text{Au}_2(\text{dppe})(\text{pdt})]$ and

$[\text{Au}_2(\text{dppn})(\text{pdt})]$ (dppn = 1,5-bis(diphenylphosphino)pentane, pdt = 1,3-propanediyldithio).²⁶ The activation energies obtained in this work are in close agreement with those reported for the dynamic process originating from an equilibrium between Au–Au-bonded and nonbonded conformations. Since **1–3** are eight- or nine-membered-ring compounds, intramolecular processes such as cis- and trans conformational isomerization or ring inversion are unlikely. Therefore the dynamic process observed in this work is likely due to an inter- and not intramolecular Au–Au bond formation. The line broadening observed for **3** at low temperature is parallel to the absorption and emission spectra, showing that molecular association occurs in solution. At a concentration of $\sim 10^{-2}$ M, the monomer/dimer ratio obtained from VT-NMR data is 1.4 (at -90 $^\circ\text{C}$) for **2**. This ratio is consistent with the value of 1.4 estimated from UV–vis spectra.

In summary, annular digold(I) compounds with diphosphine and dithiolate ligands have the tendency to aggregate in the solid state. The degree of aggregation, ranging from unassociated monomer to highly associated polymer, depends on ligands. In acetonitrile solution, intermolecular associations are also observed, as evidenced by the concentration-dependent behavior of absorption and emission spectra and variable-temperature ^{31}P NMR spectra. Concentration-dependent absorption spectra of **2** and **3** suggest that an equilibrium between monomer and dimer exists. Equilibrium constants of ~ 38 and ~ 61 M^{-1} , ΔH values of ~ 14 – 15 kcal/mol, and ΔS values of ~ -35 and ~ -46 cal/(K mol) were calculated for compounds **2** and **3**. The tendency to dimerize appears to be high. The ΔH values for the intermolecular Au–Au interaction are also relatively high, as compared to previous estimated values.²¹ Well-resolved excitation and emission spectra for monomers at a lower concentration and dimers at a higher concentration are observed for compounds **2**, **3**, and **8**. Interestingly, **3** and **8** are monomeric in the solid state but the dimeric form can be observed in solution. Although oligomerization higher than dimerization was observed in the solid state for some compounds, no molecular association higher than dimeric was observed in acetonitrile solution because of the nonrigidity of the ring compounds in solution. For this system we are able to observe four different emissions originating from (1) Au_2 ^1MC transitions for monomeric compounds in solution, (2) Au_4 ^1MC transitions for the dimers in solution, (3) a $\text{S} \rightarrow \text{Au}$ $^3\text{LMCT}$ excited state for open-ring compound **4** in a 77 K glass state, and (4) a dithiolate $\rightarrow \text{Au}$ $^3\text{LMCT}$ excited state for annular ring compounds in a 77 K glass state. The richness of luminescent behavior in this work warrants further attention.

Acknowledgment. We thank the National Science Council of Taiwan (Grants NSC 85-2113-M-031-004 and NSC85-2113-M-030-009) for financial support.

Supporting Information Available: Tables giving positional and isotropic thermal parameters, anisotropic thermal parameters, and bond lengths and angles for $[\text{Au}_2(\text{dmpm})(i\text{-mnt})]$ and $[\text{Au}_2(\text{dppe})(i\text{-mnt})]$ and figures showing the concentration dependence of UV–vis absorption and emission spectra (14 pages). Ordering information is given on any current masthead page.

IC9607245

(24) Pople, J. A.; Schneider, W. G.; Bernstein, H. J. *High-Resolution Nuclear Magnetic Resonance*; McGraw-Hill: New York, 1959; p 242.
(25) Shanan-Atidi, H.; Bar-Eli, K. H. *J. Phys. Chem.* **1970**, *74*, 961.

(26) Narayanaswamy, R.; Young, M. A.; Parkhurst, E.; Ouellete, M.; Kerr, M. E.; Ho, D. M.; Elder, R. C.; Bruce, A. E.; Bruce, M. R. M. *Inorg. Chem.* **1993**, *32*, 2506.